

Non-linear Fano Interferences in Open Quantum Systems: an Exactly Solvable Model

Daniel Finkelstein-Shapiro,^{1,2,3} Monica Calatayud,^{2,3,4} Osman Atabek,⁵ Vladimiro Mujica,¹ and Arne Keller⁵

¹*Department of Chemistry and Biochemistry, Arizona State University, Tempe AZ 85282*

²*Sorbonne Universités, UPMC Univ Paris 06, UMR 7616,*

Laboratoire de Chimie Théorique, F-75005, Paris, France

³*CNRS, UMR 7616, Laboratoire de Chimie Théorique, F-75005, Paris, France*

⁴*Institut Universitaire de France, France*

⁵*Institut des Sciences Moléculaires d'Orsay, Bâtiment 350, UMR8214, CNRS-Univ. Paris-Sud, Univ. Paris-Saclay 91405 Orsay, France*

We obtain an explicit solution for the stationary state populations of a dissipative Fano model, where a discrete excited state is coupled to a continuum set of states; both excited set of states are reachable by photo-excitation from the ground state. The dissipative dynamic is described by a Liouville equation in Lindblad form and the field intensity can take arbitrary values within the model. We show that the continuum states population as a function of laser frequency can always be expressed as a Fano profile plus a Lorentzian function with effective parameters whose explicit expressions are given in the case of a closed system coupled to a bath as well as for the original Fano scattering framework. Although the solution is intricate, it can be elegantly expressed as a linear transformation of the kernel of a 4×4 matrix which has the meaning of an effective Liouvillian. We unveil key notable processes related to the optical nonlinearity and which had not been reported to date: electromagnetic induced-transparency, population inversions, power narrowing and broadening, as well as an effective reduction of the Fano asymmetry parameter.

INTRODUCTION

The original Fano model was introduced by U. Fano in 1935 [1] and formalized in 1961 [2] to explain the asymmetry in the absorption or photo-current profile as a function of laser frequency used to ionize a gaz of Helium-like atoms [3]. Previously, similar diffuse absorption bands induced by iodine-chloride pre-dissociation have been observed and theoretically addressed [4]. Friederichs [5] developed the mathematical formalism of perturbation of linear operators to describe the essential feature of the Fano model: a discrete state coupled to a continuum set of states; both sets of states being reachable by photo-excitation from the ground state. The resulting photo-current, which is proportional to the population of the continuum set of states, as a function of the excitation laser frequency ω_L is known as the Beutler-Fano or Fano profile:

$$f(\epsilon; q) = \frac{(q + \epsilon)^2}{\epsilon^2 + 1}, \quad (1)$$

where q is the ratio of the transition dipole moment of the ground-discrete and ground-continuum transitions, and $\epsilon = (\omega_L - \omega_e)/\gamma$ where $\hbar\omega_e$ is the energy of the discrete state relative to the ground state, ω_L is the incident radiation field frequency, and $\hbar\gamma = n\pi V^2$ is the linewidth of the excited state, induced by its coupling (per unit of energy) nV^2 to the continuum set of states, n being the density of states. The Fano literature is extensive and we cannot do justice in this paper to all the contributions since 1935. The interested reader is pointed to Refs. [6–8].

Two important extensions of the original model have been considered: inclusion of incoherent relaxation and

dephasing processes and high field intensities. The motivation to include incoherent processes was first to describe the pressure broadening [9] due to elastic collisions, laser phase fluctuations [10] and spontaneous emission [11, 12]. Nowadays, Fano profiles in nanoscale structures are standard [13, 14], for example in plasmonic nanostructures [15–17], quantum dots, decorated nanoparticles [18] and spin filters [19]. The coherent coupling with the incident light induces large Rabi frequencies which in turn compete with the relaxation rates in order to modify the stationary state. The ability to predict the lineshape, and in general to investigate non linear optical phenomena in the presence of a continuum set of states are the main motivations to consider large incident field intensity. A growing number of experimental and theoretical papers have been appearing on the subject of coherent control and ultrafast pulses on Fano models [20–23].

In spite of the ubiquity of the Fano interferences, to the best of our knowledge, explicit solutions for high laser intensities and including general relaxation processes have not been obtained. Even in Refs. [24, 25], dealing with quantum dots, despite some approximations no analytical expressions are derived that afford a simple physical interpretation of the results.

In a recent work [26], we investigated the signatures of the Fano interferences in the emitted spectrum of a system with a vibrational manifold. We obtained explicit expressions of spectroscopic observables like Rayleigh, Raman and fluorescence emission but restricted to the low intensity field limit where the lowest order of perturbation was enough to describe the laser-matter interaction. In this letter, we focus on the description of the non-linear Fano effect on the total population of the con-

tinuum excited state, the observable in the original Fano model, but for the general case of large intensities of the laser field and including dissipation processes. Here, unlike Ref. [26], obtaining explicit expressions requires non perturbative calculations. We present a method that allows us to obtain such an explicit formulation for large field strengths and Markovian baths in an elegant and intuitive framework where the entire solution is formulated in terms of a 4×4 matrix corresponding to an effective Liouvillian acting in the space of the discrete states only. We calculate the usual Fano observable, that is, the total population of the continuum set of states, which is related to the optical absorption or to the photo-current, as a function of the incident laser frequency. The striking result is that such a function can be written exactly as a linear combination of a Fano profile and a Lorentzian function like in Ref. [26], but where the Fano q and ϵ coefficients become effective parameters that are functions of the field intensity and the decay rates.

MODEL

Although the objectives and results of the present work differ from our previous one [26], the model is similar. As there are some differences and for the sake of introducing the notation in a self-contained way, we summarize it below. The ingredients of the model are schematically presented in Fig. 1. The Hamiltonian $H = H_0 + H_V + H_F$ is exactly the same as in the original Fano model [2]:

$$\begin{aligned} H_0 &= E_0|g\rangle\langle g| + E_e|e\rangle\langle e| + \int dk \epsilon_k |k\rangle\langle k| \\ H_V &= \int dk V(k) |e\rangle\langle k| + V^*(k) |k\rangle\langle e| \\ H_F &= F [\mu_e \cos(\omega_L t) |g\rangle\langle e| + \mu_e^* \cos(\omega_L t) |e\rangle\langle g|] \\ &+ F \int dk [\mu_k \cos(\omega_L t) |g\rangle\langle k| + \mu_k^* \cos(\omega_L t) |k\rangle\langle g|], \quad (2) \end{aligned}$$

where H_0 is the site Hamiltonian, H_V is the coupling of the excited state to the continuum. For simplicity, in the following, we will consider that $V(k) = \langle e|H_V|k\rangle$ is real. H_F is the interaction with the incident radiation field, allowing transitions from the ground state to the discrete excited state $g \leftrightarrow e$ and to the continuum of states $g \leftrightarrow k$, $\mu_{ij} = \langle i|\mu|j\rangle$ is the transition dipole moment between states i and j and F is the field amplitude.

The relaxation and dephasing processes are introduced in an analogue way as in Ref. [26]. It consists in a Liouville equation in Lindblad form to insure complete positivity of the density matrix describing the quantum system. The dynamics of the system is given by: $\frac{\partial \rho}{\partial t} = \mathcal{L}(t)\rho$, where $\mathcal{L}(t) = \mathcal{L}_H(t) + L^D$, with $\hbar \mathcal{L}_H = -i(\mathbb{1} \otimes H(t) - \bar{H}(t) \otimes \mathbb{1})$ is the Hamiltonian conservative part, with \bar{H} the complex conjugate of H , and

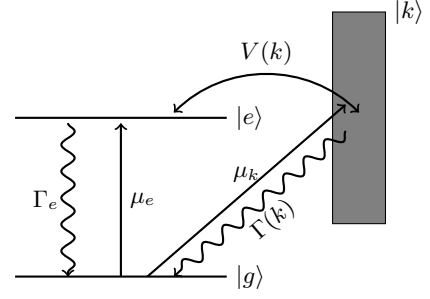


FIG. 1: Energy levels and transitions of a Fano-type model with dissipation (see main text for notations)

$L^D = L_{\text{pop}}^D + L_{\text{pure}}^D$ is the generator of dissipative dynamics.

$$\begin{aligned} L_{\text{pop}}^D &= \int dk \Gamma(k) \left\{ A(k, g) \otimes A(k, g) \right. \\ &- \frac{1}{2} [1 \otimes A^\dagger(k, g) A(k, g) + A^\dagger(k, g) A(k, g) \otimes 1] \Big\} \\ &+ \Gamma_e \left\{ A(e, g) \otimes A(e, g) \right. \\ &- \frac{1}{2} [1 \otimes A^\dagger(e, g) A(e, g) + A^\dagger(e, g) A(e, g) \otimes 1] \Big\}, \quad (3) \end{aligned}$$

describes the population relaxation from the $|k\rangle$ manifold and from the $|e\rangle$ state to the ground state.

$$\begin{aligned} L_{\text{pure}}^D &= -\gamma_{eg} [|e\rangle\langle e| \otimes |g\rangle\langle g| + |g\rangle\langle g| \otimes |e\rangle\langle e|] \\ &- \int dk \gamma_{kg} [|k\rangle\langle k| \otimes |g\rangle\langle g| + |g\rangle\langle g| \otimes |k\rangle\langle k|] \\ &- \int dk \gamma_{ke} [|k\rangle\langle k| \otimes |e\rangle\langle e| + |e\rangle\langle e| \otimes |k\rangle\langle k|], \quad (4) \end{aligned}$$

describes pure dephasing, that is the dynamics of the non diagonal matrix elements of ρ . $A(i, j) = |j\rangle\langle i|$ are the jump operators and $\Gamma(k)$ is the population relaxation rate from state $|k\rangle$ to $|g\rangle$ as is Γ_e for the $|e\rangle$ population. γ_{ij} is the pure dephasing rate for the ij coherence. As in Ref. [26], we have used the correspondence: $|l\rangle\langle m| \leftrightarrow |l\rangle \otimes |m\rangle \equiv ||lm\rangle$ [27]. We use the rotating-wave approximation (RWA) on $L = e^{i\Omega_L t} \mathcal{L}(t) e^{-i\Omega_L t}$ and remove non-resonant terms such that L can be considered time independent. Ω_L is a diagonal matrix whose matrix elements are equal to $\pm\omega_L$ for excited(ground)-ground(excited) coherences, and zero elsewhere.

There are a number of phenomena that occur at strong fields which are not described by the present model (ATI, continuum-continuum transitions). This is in line with previous literature where these processes are also neglected from the model. Within these assumptions, the only restriction of the model is that the Rabi frequency should be much smaller than the laser frequency, which is around the two-level system (TLS) transition as we consider near resonant processes. This is once more an approximation done throughout the literature. This is not restrictive since all the high-field effects described by

the model appear at field intensities that are a few percent of the intensities at which the RWA breaks down for a TLS in the visible and a linewidth of around 0.1 eV. In this context, it is the comparison between the laser intensity or more precisely the Rabi frequency and relaxation rates that determines the limit between the linear and nonlinear regime.

FESHBACH PARTITIONING AND EFFECTIVE LIOUVILLIAN

The continuum states population, $\int dk \rho_{kk}$, where ρ is the full steady state density matrix can be obtained by finding the kernel of the time-independent operator $(\underline{\Omega}_L - L)$, that is $(\underline{\Omega}_L - L)\rho = 0$. To solve this equation, we split L in two terms, $L = L_0 + \mathcal{V}$ where L_0 is diagonal and \mathcal{V} is purely non diagonal, and proceed to Feshbach partitioning [28]. For that, we introduce the projectors $P = |g\rangle\langle g| + |e\rangle\langle e|$ and $Q = \int dk |k\rangle\langle k|$, with $P + Q = 1$. The corresponding projectors for the discrete and continuum parts in Liouville space are given by:

$$\mathcal{P} = P \otimes P; \quad \mathcal{Q} = P \otimes Q + Q \otimes P + Q \otimes Q. \quad (5)$$

This allows us to rewrite the kernel equation as $(\underline{\Omega}_L - L)(\mathcal{P} + \mathcal{Q})\rho = 0$. By projecting on both \mathcal{P} and \mathcal{Q} and after some algebra (see Appendix A), we obtain

$$\mathcal{P}(\underline{\Omega}_L - L_{\text{eff}})\mathcal{P}\rho = 0, \quad (6)$$

with an effective Liouville operator,

$$L_{\text{eff}} = \mathcal{P}L\mathcal{P} + \mathcal{P}\mathcal{V}\mathcal{Q}\mathcal{G}_Q\mathcal{Q}\mathcal{V}\mathcal{P}, \quad (7)$$

and $\mathcal{G}_Q = (\mathcal{Q}(\underline{\Omega}_L - L)\mathcal{Q})^{-1}$. \mathcal{G}_Q , which is related to the resolvent of $\mathcal{Q}L\mathcal{Q}$, is not straightforward to calculate unless $\mathcal{Q}L\mathcal{Q}$ is diagonal. To achieve the calculation of \mathcal{G}_Q , we proceed to a sub-partition of the \mathcal{Q} subspace until the projected Liouvillian be diagonal (see Appendix A). $\mathcal{P}\underline{\Omega}_L\mathcal{P} - L_{\text{eff}}$ acts on the \mathcal{P} space only, but its kernel is equal to the projection $P\rho$ of the exact stationary density matrix, on the discrete subspace. Once the density matrix $\mathcal{P}\rho$ on the discrete space has been obtained, the density matrix $\mathcal{Q}\rho$ in the continuum subspace can be computed through the following equation:

$$\mathcal{Q}\rho = \mathcal{Q}\mathcal{G}_Q\mathcal{Q}\mathcal{V}\mathcal{P}\rho. \quad (8)$$

L_{eff} can be thought as a 4×4 matrix when $\mathcal{P}\rho$ is considered as a column vector with 4 elements. To obtain an explicit expression for L_{eff} , the usual wide-band approximation is employed. It is also in this same approximation that an explicit expression was obtained in the original Fano problem [2]. It consists in assuming that the parameters of the model do not depend upon k . From now on, we consider this approximation and define $\Gamma_c \equiv \Gamma(k)$, $\mu_c \equiv \mu_k$ as constants.

After tedious but straightforward calculations (see Appendix A), the effective Liouvillian L_{eff} defined in Eq. (6) can be written in a surprisingly simple form:

$$L_{\text{eff}} = -i(\mathbb{1} \otimes H_{\text{eff}} - \bar{H}_{\text{eff}} \otimes \mathbb{1}) + L_{\text{eff}}^D, \quad (9)$$

where H_{eff} is an effective Hamiltonian and L_{eff}^D is the dissipative part of the effective Liouvillian. We show explicitly in Appendix B that L_{eff} has a Lindblad form. It can thus be considered as the generator of complete positive evolution. This ensure that its kernel $P\rho$ is indeed a physical state. Here, we prefer a different presentation of the operator that makes it more amenable for comparison to the effective Hamiltonian that is calculated in the scattering problem where dissipation is ignored. The effective Hamiltonian can be written as:

$$H_{\text{eff}} = PH_0P + H_{\text{field}}, \text{ with} \quad (10)$$

$$H_{\text{field}} = \frac{F}{2}(\mu_e - in\pi V\mu_c)(|g\rangle\langle e| + |e\rangle\langle g|).$$

It contains an Hermitian and an anti-Hermitian part and corresponds exactly to the effective Hamiltonian of typical resonance problems in Hilbert space [29, 30]. The non-Hamiltonian part of the effective Liouvillian is:

$$L_{\text{eff}}^D = L_e^D + L_c^D + L_{\text{pure}}^D, \text{ with:}$$

$$\hbar L_e^D = (2n\pi V^2 + \hbar\Gamma_e) \left[A(e, g) \otimes A^\dagger(e, g) - \frac{1}{2} \left(A^\dagger(e, g)A(e, g) \otimes 1 + 1 \otimes A^\dagger(e, g)A(e, g) \right) \right]$$

$$L_{\text{pure}}^D = -(\gamma_{eg} + n\pi\mu_c^2)[|e\rangle\langle e| \otimes |g\rangle\langle g| + |g\rangle\langle g| \otimes |e\rangle\langle e|]$$

$$\hbar L_c^D = 2n\pi V\mu_c(|gg\rangle\langle eg| + |eg\rangle\langle gg|) \quad (11)$$

L_e^D is a dissipation superoperator in Lindblad form that describes the population decay with rate $2n\pi V^2/\hbar + \Gamma_e$ due to the coupling to the continuum and the natural decay rate Γ_e , and L_{pure}^D is a pure dephasing superoperator. L_c^D is an additional part of the relaxation superoperator which cannot be put into a Lindblad form. We stress that this presentation allows a comparison to the Hilbert space solution but that the full L_{eff} operator of Eq. (9) can be put in Lindblad form (see Appendix B).

Finally, solving Eqs. (6) amounts to finding the kernel of a 4×4 matrix, which can be explicitly done with the help of a symbolic calculation software (see Appendix C). Then, applying Eq. (8) along with the normalization condition $\rho_{gg} + \rho_{ee} + \int dk \rho_{kk} = 1$ gives us all of the populations and coherences.

The results will be given in terms of dimensionless quantities and $\hbar\gamma = n\pi V^2$ is taken as the unit of energy. In addition to the original dimensionless Fano parameters $\epsilon = (\omega_L - \omega_e)/\gamma$ and $q = \mu_e/n\pi V\mu_c$, we introduce the new parameter $\Omega = \frac{\mu_e F}{2q\hbar\gamma} = \mu_c F/2V$, which corresponds to a dimensionless Rabi frequency. Also, all relaxation

rates will be given in units of γ , this amounts to perform the following replacement: $\Gamma_c \rightarrow \Gamma_c/\gamma$, $\Gamma_e \rightarrow \Gamma_e/\gamma$, $\gamma_{eg} \rightarrow \gamma_{eg}/\gamma$.

GENERALIZED FANO PROFILE WITH DISSIPATION

The main result of the paper is that the population of the excited state $n_c = \int dk \rho_{kk}$ can always be brought back to a Fano profile f , plus a Lorentzian term:

$$n_c(\epsilon_{\text{eff}}; q_{\text{eff}}) = C \left[f(\epsilon_{\text{eff}}; q_{\text{eff}}) + \frac{D}{\epsilon_{\text{eff}}^2 + 1} \right], \quad (12)$$

where the dependence upon ω_L is solely contained in $\epsilon_{\text{eff}} = \frac{\omega_L - \omega_{\text{eff}}}{\gamma_{\text{eff}}}$. ω_{eff} , γ_{eff} and q_{eff} are effective Fano parameters that depend on all the parameters of the model but ω_L . C is a measure of the total population and D

indicates the relative weight of the Lorentzian term in comparison to the Fano profile. The transformation into the above form involves a rescaling of the parameters achieved in the accompanying software (see Appendix C).

Simple explicit expressions for the effective Fano parameters can be given when the relaxation and the dephasing rates concerning the $|e\rangle$ state can be neglected, that is when $\Gamma_e = 0$ and $\gamma_{eg} = 0$ (see Eq. (13)). This is often a very good approximation in the context of semiconductor quantum dots or in hybrids consisting of an organic molecule adsorbed on metallic or semiconductor nanoparticles [31–35] ($1/\Gamma_e \approx$ nanoseconds, $\hbar/n\pi V^2 \approx 10$ femtoseconds). In that case, the only relaxation process consists in the continuum states population decay to the ground state and the profile is given by a pure Fano profile and the Lorentzian term is absent, $D = 0$ and $C = \frac{2\Omega^2}{2\Omega^2 + \Gamma_c}$. We have obtained:

$$\begin{aligned} \frac{\gamma_{\text{eff}}}{\gamma} &= \frac{\Gamma_c [1 + (q^2 + 1)\Omega^2((2\Omega^2 + 4)/\Gamma_c + 1) + 2/\Gamma_c + 2]^{1/2}}{2\Omega^2 + \Gamma_c} \\ \frac{\omega_{\text{eff}}}{\gamma} &= \frac{\omega_e}{\gamma} + q\Omega^2 \left(1 - \frac{2}{2\Omega^2 + \Gamma_c} \right); \quad \frac{q_{\text{eff}}}{q} = \frac{\Gamma_c}{2\Omega^2 + \Gamma_c} \frac{1}{\gamma_{\text{eff}}}. \end{aligned} \quad (13)$$

We now discuss each one of the parameters as a function of the Rabi frequency and illustrate them in Figure 2. We note that these parameters have a non-linear dependence on the Rabi frequency Ω , or in other words, a non-linear dependence on the strength of the field. The prefactor C which is proportional to the intensity of the field for weak fields (linear regime) saturates to $C = 1$ when $2\Omega^2 \gg \Gamma_c$. In Fig. 2a, we show the normalized Fano profiles at two intensities of the field ($\Omega = 0.001$ and $\Omega = 0.1$ for $q = 5$). As the field intensity increases, we see changes in all of the Fano parameters. The effective width γ_{eff} increases or decreases (power narrowing or power broadening) depending on the value of the relaxation (see Fig. 2b and Eq. (13)). The effective asymmetry parameter q_{eff} decreases monotonically with q (see Figure 2c and Eq. (13)). As shown in the inset, the population of the continuum, even for modest values of Ω is significant, underlying the importance of a theory which can handle non-negligible population in the continuum set of states, contrary to the approximations in Ref. [25]. The decrease of q_{eff} can be thought as a consequence of the saturation of the discrete excited state population. The energy shift $\hbar(\omega_{\text{eff}} - \omega_e)$ of the discrete state $|e\rangle$, that can be seen as an AC Stark shift, has an interesting behavior. For $\Gamma_c < 2$, the shift is negative if $0 < \Omega < \sqrt{(2 - \Gamma_c)/2}$ and

it is positive if $\Omega > \sqrt{(2 - \Gamma_c)/2}$. Therefore, $\Gamma_c < 2$, $\Omega = \sqrt{(2 - \Gamma_c)/2}$ is a null point. On the contrary, for large relaxation rates such that $\Gamma_c > 2$, the shift will be positive for all values of the field (see Fig. 2d).

Inclusion of population relaxation ($\Gamma_e \neq 0$) or pure dephasing processes ($\gamma_{eg} \neq 0$) results into heavy expressions of the states populations that we provide in the accompanying software (see Appendix C). The main qualitative features remain unchanged except for the appearance of a Lorentzian term.

Until now, we have focused on the stationary population of the continuum set of states $\int dk \rho_{kk}$. Another quantity that can be measured is the photocurrent, that is the total flow of electrons in the continuum. Assuming that all the electrons emitted in the continuum $|k\rangle$ states are collected by an electrode, in the limit of low bias voltage, the current intensity I can be obtained from the stationary populations as $I = \lim_{\Gamma_c \rightarrow 0} |e| \frac{\Gamma_c \int dk \rho_{kk}}{\rho_{gg}}$ [36], where e is the electron charge. It turns out that I can also be brought into the form of a Fano factor and a Lorentzian factor as in equation (12). Explicit expressions for the Fano and Lorentzian parameters can be given with both the population relaxation and dephasing included:

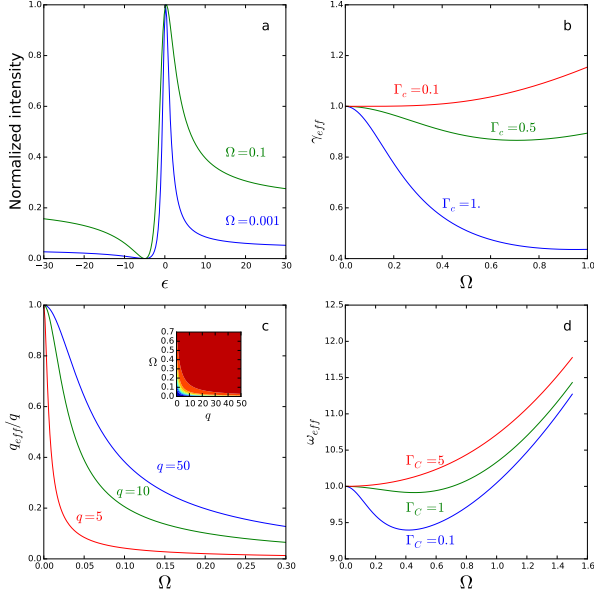


FIG. 2: Effect of the field on the Fano profiles and parameters: (a) Fano profiles for $q = 5$ for $\Omega = 0.001$ and $\Omega = 0.1$ (b) γ_{eff} for different values of Γ_e (c) q_{eff}/q for different values of q . Inset show n_c as a function of q and Ω . Upper end (red) corresponds to $n_c = 1$ and lower end (blue) corresponds to $n_c = 0$ (d) ω_{eff} for different values of Γ_c and $\omega_e = 10$

$$\gamma_{\text{eff}}^{\text{tr}} = (1 + \Gamma_e)^{-1} \left[\Omega^4 \Gamma_e (q^2 + \Gamma_e + 1) + \Omega^2 (1 + \Gamma_e) (q^2 + 2\Gamma_e + 1) (\Gamma_e + \gamma_{eg} + 1) + (1 + \Gamma_e)^2 (\Gamma_e + \gamma_{eg} + 1)^2 \right]^{1/2} \quad (14)$$

$$D^{\text{tr}} = \frac{1}{(\gamma_{\text{eff}}^{\text{tr}})^2} (1 + \Gamma_e)^{-2} \left[\Omega^4 \Gamma_e (q^2 + \Gamma_e + 1) + \Omega^2 (1 + \Gamma_e) (q^2 + 2\Gamma_e + 1) (\Gamma_e + \gamma_{eg}) \right] \\ + \frac{1}{(\gamma_{\text{eff}}^{\text{tr}})^2} (1 + \Gamma_e)^{-1} \left[\Gamma_e^3 + \Gamma_e^2 + \gamma_{eg} (2\Gamma_e^2 + \Gamma_e \gamma_{eg} + q^2 + 2\Gamma_e + \gamma_{eg} + 1) \right], \quad (15)$$

$$\frac{\omega_{\text{eff}}^{\text{tr}}}{\gamma} = \frac{\omega_e}{\gamma} + \frac{q\Omega^2}{1 + \Gamma_e}; \quad q_{\text{eff}}^{\text{tr}} = \frac{1}{\gamma_{\text{eff}}^{\text{tr}}}; \quad C^{\text{tr}} = 2\Omega^2. \quad (16)$$

These expressions give an exact description of the scattering problem, as formulated by Fano in its original work [2], but extended to large field intensities and dissipation processes.

An interesting consequence of the nonlinear Fano effect, is electromagnetically-induced transparency (EIT) [37]. Indeed, in the absence of discrete state relaxation and dephasing ($\Gamma_e = \gamma_{eg} = 0$), then $D^{\text{tr}} = 0$ in Eq. (15) and therefore the continuum population goes through zero when $\epsilon_{\text{eff}} = -q_{\text{eff}}$ (see Eq. (12)). The phenomenon of EIT has been characterized before [38, 39]. In the standard scheme, EIT is obtained with two laser frequencies, where one acts as the control radiation that creates the transparency window while the second one acts as a probe. In our case, which is non-standard, the same frequency acts as a control and

probe radiation, and the transparency window arises from two pathways whose destructive interference point is tunable via its intensity. It can be shown that the condition $\epsilon_{\text{eff}} = -q_{\text{eff}}$ is equivalent to $\Omega^2 = 1 + \frac{\epsilon}{q}$ either for the light absorption or the photocurrent intensity. This phenomenon is shown in Fig. 3.a for the case $\epsilon = 0$, $q = 15$ for different values of Γ_e , and Fig. 3.b $\Gamma_e = 0$ for different values of ϵ . This phenomenon provides an interesting tool for devices as well as a means for determining the system parameters. For example, irradiating at the discrete level resonance ($\epsilon = 0$) in weak field and increasing the intensity until the induced transparency is found determines the ratio of transition dipole moment μ_c to the coupling V such that $\mu_c/2V = 1/F$. In the presence of pure dephasing or of relaxation from the discrete state, the zero becomes a minimum but its position does not change appreciably (see Figure 3 (left)). One should take care not to confuse

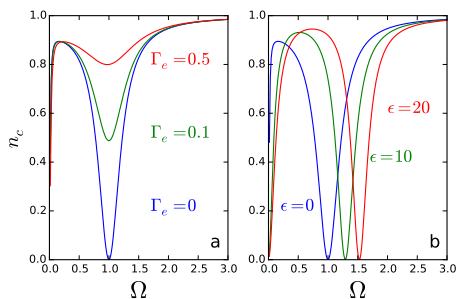


FIG. 3: Population in the continuum showing electromagnetically induced transparency (EIT) for a) $\epsilon = 0$, $q = 15$ with different values of Γ_e and b) for $q = 15$, $\Gamma_e = 0$ different values of ϵ

the present effect with the trivial zero of the standard Fano profile at $\epsilon = -q$ (see Eq. (1)). In the case presented here, the effect is non-linear as the condition is $\epsilon_{\text{eff}} = -q_{\text{eff}}$ and both of these parameters depend non-linearly on the field. The condition for the minimum is thus obtained by adjusting the intensity of the field.

CONCLUSION

We have obtained an explicit formula solving the original Fano problem for arbitrary relaxation processes and large radiative couplings. The inclusion of more than a single excited discrete state is straightforward as long as the couplings do not exceed the energy gap between excited states. Furthermore, our approach serves as a stepping stone for descriptions going beyond the wide-band approximation, already discussed in the scattering framework. Finally, there is a wide class of systems where the present model is directly applicable opening new horizons in the analysis of Fano profiles under intense fields, as well as in applications and devices that exploit processes such as population inversion and electromagnetically induced transparency.

Acknowledgements D.F.S. acknowledges the Research in Paris program for a fellowship and Victoria Cantoral Farfan and Sadek Salem Al Harbat (UPMC) for fruitful discussions. This work was financially supported by project NSF-ANR (ANR-11-NS04-0001 FRAMOLSENT program, NSFCHE-112489). This work was performed using HPC resources from GENCI- CINES/IDRIS (Grant 2015- x2015082131, 2014- x2014082131) and the CCRE-DSI of Université P. M. Curie.

[1] U. Fano, *Il Nuovo Cimento* **12**, 154 (1935).
 [2] U. Fano, *Phys. Rev.* **124**, 1866 (1961).

[3] H. Beutler, *Zeitschrift für Physik* **93**, 177 (1935).
 [4] O. K. Rice, *The Journal of Chemical Physics* **1**, 375 (1933).
 [5] K. O. Friedrichs, *Commun. Pure Appl. Math.* **1**, 361 (1948).
 [6] U. Fano, *Atomic Collisions and Spectra* (Elsevier Science, 2012).
 [7] S. Satpathy, A. Roy, and A. Mohapatra, *European Journal of Physics* **33**, 863 (2012).
 [8] A. R. P. Rau, *Physica Scripta* **69**, C10 (2004).
 [9] U. Fano, *Phys. Rev.* **131**, 259 (1963).
 [10] K. Rzażewski and J. H. Eberly, *Phys. Rev. A* **27**, 2026 (1983).
 [11] G. S. Agarwal, S. L. Haan, K. Burnett, and J. Cooper, *Phys. Rev. Lett.* **48**, 1164 (1982).
 [12] F. Robicheaux, T. W. Gorczyca, M. S. Pindzola, and N. R. Badnell, *Phys. Rev. A* **52**, 1319 (1995).
 [13] A. E. Miroshnichenko, S. Flach, and Y. S. Kivshar, *Rev. Mod. Phys.* **82**, 2257 (2010).
 [14] M. Rahmani, B. Luk'yanchuk, and M. Hong, *Laser & Photonics Reviews* **7**, 329 (2013).
 [15] T. Pakizeh, C. Langhammer, I. Zori, P. Apell, and M. Kil, *Nano Lett.* **9**, 882 (2009).
 [16] B. Lukyanchuk, N. I. Zheludev, S. A. Maier, N. J. Halas, P. Nordlander, H. Giessen, and C. T. Chong, *Nat. Mater.* **9**, 707 (2010).
 [17] C. W. Hsu, B. G. DeLacy, S. G. Johnson, J. D. Joannopoulos, and M. Soljacic, *Nano Lett.* **14**, 2783 (2014).
 [18] J. R. Lombardi and R. L. Birke, *J. Phys. Chem. C* **114**, 7812 (2010).
 [19] J. F. Song, Y. Ochiai, and J. P. Bird, *Appl. Phys. Lett.* **82**, 4561 (2003).
 [20] C. Ott, A. Kaldun, P. Raith, K. Meyer, M. Laux, J. Evers, C. H. Keitel, C. H. Greene, and T. Pfeifer, *Science* **340**, 716 (2013).
 [21] W.-C. Chu and C. D. Lin, *Phys. Rev. A* **82**, 053415 (2010).
 [22] M. Wickenhauser, J. Burgdörfer, F. Krausz, and M. Drescher, *Phys. Rev. Lett.* **94**, 023002 (2005).
 [23] Z.-H. Loh and S. R. Leone, *The Journal of Physical Chemistry Letters* **4**, 292 (2013), pMID: 26283437.
 [24] M. Kroner, A. O. Govorov, S. Remil, B. Biedermann, S. Seidl, P. M. Badolato, A. ad Petroff, W. Zhang, R. Barbour, B. D. Gerardot, R. J. Warburton, and K. K., *Nature* **451**, 311 (2008).
 [25] W. Zhang and A. O. Govorov, *Phys. Rev. B* **84**, 081405 (2011).
 [26] D. Finkelstein-Shapiro, I. Urdaneta, M. Calatayud, O. Atabek, V. Mujica, and A. Keller, *Phys. Rev. Lett.* **115**, 113006 (2015).
 [27] T. F. Havel, *Journal of Mathematical Physics* **44**, 534 (2003).
 [28] H. Feshbach, *Annals of Physics* **19**, 287 (1962).
 [29] R. Bertlmann, W. Grimus, and B. Hiesmayr, *Phys. Rev. A* **73**, 054101 (2006).
 [30] N. Moiseyev, *Non-Hermitian Quantum Mechanics* (Cambridge University Press, 2011).
 [31] S. Raymond, X. Guo, J. L. Merz, and S. Fafard, *Phys. Rev. B* **59**, 7624 (1999).
 [32] D. Hessman, P. Castrillo, M. Pistol, C. Pryor, and L. Samuelson, *Appl. Phys. Lett.* **69**, 749 (1996).
 [33] N. Turro, *Modern Molecular Photochemistry* (University Science Books, 1991).

- [34] P. Piotrowiak, E. Galoppini, Q. Wei, G. J. Meyer, and P. Wiewior, *J. Am. Chem. Soc.* **125**, 5278 (2003).
- [35] A. Petersson, M. Ratner, and H. O. Karlsson, *J. Phys. Chem. B* **104**, 8498 (2000).
- [36] W. B. Davis, M. R. Wasielewski, M. A. Ratner, V. Mujica, and A. Nitzan, *J. Phys. Chem. A* **101**, 6158 (1997).
- [37] K.-J. Boller, A. Imamoğlu, and S. E. Harris, *Phys. Rev. Lett.* **66**, 2593 (1991).
- [38] C. Buth, R. Santra, and L. Young, *Phys. Rev. Lett.* **98**, 253001 (2007).
- [39] T. E. Glover, M. P. Hertlein, S. H. Southworth, T. K. Allison, J. van Tilborg, E. P. Kanter, B. Krassig, H. R. Varma, B. Rude, R. Santra, A. Belkacem, and L. Young, *Nat Phys* **6**, 69 (2010).
- [40] G. Lindblad, *Communications in Mathematical Physics* **48**, 119 (1976).
- [41] V. Gorini, A. Kossakowski, and E. C. G. Sudarshan, *Journal of Mathematical Physics* **17**, 821 (1976).

APPENDIX A: STEADY-STATE DENSITY MATRIX

We outline the procedure used to obtain the steady-state density matrix by finding the kernel of $\underline{\Omega}_L - L$. This process can be separated into two different equations, one for the discrete subspace and one for the continuum subspace. The density matrix in the discrete subspace $\mathcal{P}\rho$ is the solution to:

$$[\underline{\Omega}_L - (\mathcal{P}L\mathcal{P} + \mathcal{P}\mathcal{V}\mathcal{Q}\mathcal{G}_\mathcal{Q}\mathcal{Q}\mathcal{V}\mathcal{P})]\rho = 0 \quad (17)$$

The density matrix in the continuum subspace $\mathcal{Q}\rho$ can then be calculated:

$$\mathcal{Q}\rho = \mathcal{Q}\mathcal{G}_\mathcal{Q}\mathcal{Q}\mathcal{V}\mathcal{P}\rho. \quad (18)$$

The derivation of these equations is presented below. Solving them requires the calculation of the kernel of a 4×4 matrix, which we will do with a symbolic calculator and knowledge of the resolvent $\mathcal{Q}\mathcal{G}_\mathcal{Q}\mathcal{Q} = (z + \mathcal{Q}(\underline{\Omega}_L - L)\mathcal{Q})^{-1}|_{z=0}$. In what follows we will omit z altogether since all of the expressions for the density matrix require evaluation of the resolvent for $z = 0$. There are problems arising from this inversion because the operator in parenthesis is infinite dimensional with a continuous spectrum. However, we can partition this equation successively until we arrive at a partition where the Liouvillian is diagonal. The resolvent of a diagonal matrix is trivial and this will be the cornerstone of the rest of the calculation which will use exact resummations of perturbative expansions given by the Lippman-Schwinger equation.

In the case of a Fano-type model, we use three partition spaces which are schematically represented in Figure 4.

- $P = ||gg\rangle\langle gg| + ||ge\rangle\langle ge| + ||eg\rangle\langle eg| + ||ee\rangle\langle ee|$
- $P_2 = \int dk ||kg\rangle\langle kg| + ||gk\rangle\langle gk|$

- $P_3 = \int dk ||ke\rangle\langle ke| + ||ek\rangle\langle ek|$
- $Q_3 = \int dk \int dk' ||kk'\rangle\langle kk'|$

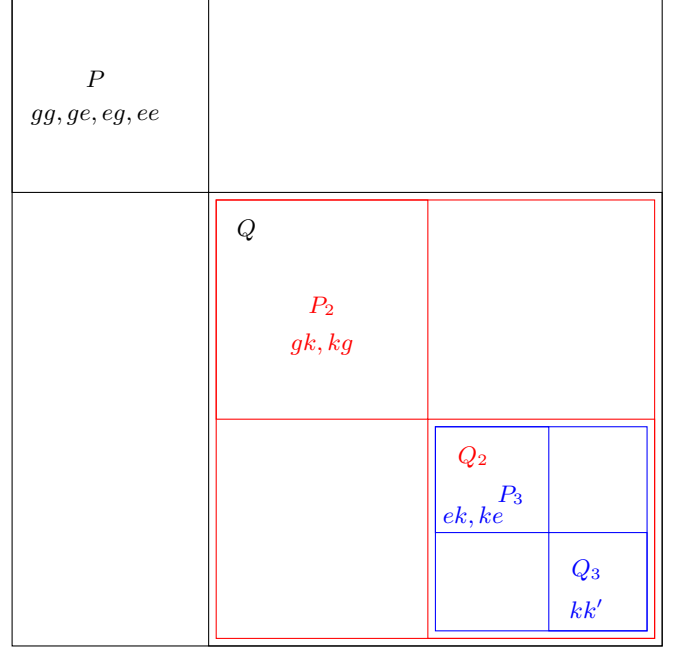


FIG. 4: Partition of the Liouvillian superoperator

The first partition divides the continuum from the discrete states and the remaining partitions divide the continuum subspace such that P_2 , P_3 and Q_3 are diagonal. A Lippman-Schwinger recursion equation applied to the last partition Q_3 and P_3 gives $Q_2\mathcal{G}_{Q_2}Q_2$, a Lippman-Schwinger equation applied to the second partition gives $\mathcal{Q}\mathcal{G}_\mathcal{Q}\mathcal{Q}$ and a third and final Lippman-Schwinger equation yields the resolvent in the entire Liouville space \mathcal{G} .

Taking the upper partition as an example, we show the expressions to calculate the resolvent. We assume that $\mathcal{Q}\mathcal{G}_\mathcal{Q}\mathcal{Q} = (\mathcal{Q}(\underline{\Omega}_L - L)\mathcal{Q})^{-1}$ and $\mathcal{P}\mathcal{G}_\mathcal{Q}\mathcal{P} = (\mathcal{P}(\underline{\Omega}_L - L)\mathcal{P})^{-1}$ are known from the previous recursion step. We also write the non-diagonal part as $\mathcal{P}L\mathcal{Q} + \mathcal{Q}L\mathcal{P} = \mathcal{V}$. We decompose the Lippman-Schwinger equation $\mathcal{G} = \mathcal{G}_0 + \mathcal{G}_0\mathcal{V}\mathcal{G}$ into its partitions. We insert $1 = \mathcal{P} + \mathcal{Q}$ on both sides of \mathcal{V} and project the entire expressions onto \mathcal{P} and \mathcal{Q} . After some rearranging:

$$\begin{aligned} \mathcal{P}\mathcal{G}\mathcal{P} &= \mathcal{P}\mathcal{G}_0\mathcal{P} + \mathcal{P}\mathcal{G}_0\mathcal{P}(\mathcal{P}\mathcal{V}\mathcal{Q}\mathcal{G}_\mathcal{Q}\mathcal{Q}\mathcal{V}\mathcal{P})\mathcal{P}\mathcal{G}\mathcal{P} \\ \mathcal{Q}\mathcal{G}\mathcal{P} &= \mathcal{Q}\mathcal{G}_0\mathcal{Q}\mathcal{V}\mathcal{P}\mathcal{G}\mathcal{P} \\ \mathcal{P}\mathcal{G}\mathcal{Q} &= \mathcal{P}\mathcal{G}\mathcal{P}\mathcal{P}\mathcal{V}\mathcal{Q}\mathcal{G}_0\mathcal{Q} \\ \mathcal{Q}\mathcal{G}\mathcal{Q} &= \mathcal{Q}\mathcal{G}_0\mathcal{Q} + \mathcal{Q}\mathcal{G}_0\mathcal{Q}\mathcal{V}\mathcal{P}\mathcal{G}\mathcal{P}\mathcal{V}\mathcal{Q}\mathcal{G}_0\mathcal{Q} \end{aligned} \quad (19)$$

We can explain more explicitly, why equations (19) solves the problem: the first equation give $\mathcal{P}\mathcal{G}\mathcal{P}$ by the inversion (or an infinite resummation) in \mathcal{P} space-we can give the explicit equation, and the other equations give the others projections in term of $\mathcal{P}\mathcal{G}\mathcal{P}$.

In our aim to obtain the steady-state density matrix, we do not need to calculate $\mathcal{P}\mathcal{G}\mathcal{P}$ but only $\mathcal{P}\mathcal{V}\mathcal{Q}\mathcal{G}_0\mathcal{Q}\mathcal{V}\mathcal{P}$. The steady-state density matrix is obtained by $(\underline{\Omega}_L - L)\rho = 0$. We can project onto \mathcal{P} and \mathcal{Q} :

$$\begin{aligned}\mathcal{P}(\underline{\Omega}_L - L)\mathcal{P}\rho + \mathcal{P}(\underline{\Omega}_L - L)\mathcal{Q}\rho &= 0 \\ \mathcal{Q}(\underline{\Omega}_L - L)\mathcal{P}\rho + \mathcal{Q}(\underline{\Omega}_L - L)\mathcal{Q}\rho &= 0\end{aligned}\quad (20)$$

which can be rearranged to get:

$$\begin{aligned}[\mathcal{P}(\underline{\Omega}_L - L)\mathcal{P} \\ - \mathcal{P}\mathcal{V}\mathcal{Q}(\mathcal{Q}(\underline{\Omega}_L - L)\mathcal{Q})^{-1}\mathcal{Q}\mathcal{V}\mathcal{P}]\rho &= 0\end{aligned}\quad (21)$$

and

$$\mathcal{Q}\rho = [(\mathcal{Q}(\underline{\Omega}_L - L)\mathcal{Q})^{-1}\mathcal{Q}\mathcal{V}\mathcal{P}]\rho \quad (22)$$

We recognize that we can group the terms in Equation (21) into an effective Liouvillian L_{eff}

$$L_{\text{eff}} = \mathcal{P}L\mathcal{P} + \mathcal{P}\mathcal{V}\mathcal{Q}\mathcal{G}_0\mathcal{Q}\mathcal{V}\mathcal{P} \quad (23)$$

where $\mathcal{G}_0 = (\mathcal{Q}(\underline{\Omega}_L - L)\mathcal{Q})^{-1}$, leading to expression (5) and (6) of the main text. To illustrate the procedure we show the calculation of the resolvent for the subspace $\mathcal{P}_3 + \mathcal{Q}_3 = \mathcal{Q}_2$. We start with the first line of Eq. (19) which gives the solution for the resolvent in the $\mathcal{P}_3\mathcal{P}_3$ subspace. We can rewrite it in the form of an infinite series $\mathcal{P}_3\mathcal{G}\mathcal{P}_3 = \mathcal{P}_3\mathcal{G}_0\mathcal{P}_3 \sum_{n=0}^{\infty} (\mathcal{P}_3\mathcal{V}\mathcal{Q}_3\mathcal{G}_0\mathcal{Q}_3\mathcal{V}\mathcal{P}_3\mathcal{G}_0\mathcal{P}_3)^n$. We denote the argument which is exponentiated inside the sum as w_3 .

$$\begin{aligned}w_3 = & - \int dk V^2 g(k, k') g(k, e) ||ke\rangle\langle ke|| \\ & - \int dk V^2 g(k', k) g(e, k) ||ek\rangle\langle ek|| \\ & \int dk \int dk' V^2 g(k', k) g(e, k) ||k'e\rangle\langle ek|| \\ & \int dk \int dk' V^2 g(k, k') g(k, e) ||ek'\rangle\langle ke||\end{aligned}\quad (24)$$

where $g(a, b) = [-i((\underline{\Omega}_L)_{ab} - E_a + E_b) + \Gamma_{ab}]^{-1}$, and Γ_{ab} is the dissipative term of the $||ab\rangle$ element of the density matrix. We need to take the geometric series of term w_3 . In the wideband approximation, the only terms which will contribute to the final result give for $\mathcal{P}_3(\mathcal{Q}_2(\underline{\Omega}_L - L)\mathcal{Q}_2)^{-1}\mathcal{P}_3$:

$$\begin{aligned}\mathcal{P}_3(\mathcal{Q}_2(\underline{\Omega}_L - L)\mathcal{Q}_2)^{-1}\mathcal{P}_3 = & \frac{g(k, e)}{1 + n\pi V^2 g(k, e)} ||ke\rangle\langle ke|| \\ & + \frac{g(e, k)}{1 + n\pi V^2 g(e, k)} ||ek\rangle\langle ek||\end{aligned}\quad (25)$$

this amounts to a renormalization which introduces an effective dissipation term - and thus linewidth - of $n\pi V^2$

to the ek and ke coherences due to the coupling of the discrete excited state with the continuum set of states. This term appears in the final effective Liouvillian as a Lindblad dissipation from the discrete excited state to the ground state with rate $2n\pi V^2/\hbar$. For a more detailed description of the integrals and their evaluation see Supplemental Information of [26].

APPENDIX B: LINDBLAD FORM OF THE EFFECTIVE LIOUVILLIAN

We now write the effective Liouvillian (Eq. (9)) in Lindblad form. Lindblad [40] and Gorini, Kowassaowki and Sudarshan [41] showed that the most general form of a Markovian process was described by a semigroup. This ensures complete positivity and trace-preserving properties of the dynamical map. The Lindblad-GKS form is:

$$L = -i[H, \rho] + \frac{1}{2} \sum_{i,j=1}^{N^2-1} c_{ij} ([F_i, \rho F_j^*] + [F_i \rho, F_j^*]) \quad (26)$$

where F_i 's form a traceless orthonormal set, H is a self-adjoint operator and c_{ij} is a positive definite matrix. We choose as the basis the Pauli matrices:

$$\sigma_x = \frac{1}{\sqrt{2}} \begin{bmatrix} 0 & 1 \\ 1 & 0 \end{bmatrix}, \sigma_y = \frac{1}{\sqrt{2}} \begin{bmatrix} 0 & i \\ -i & 0 \end{bmatrix}, \sigma_z = \frac{1}{\sqrt{2}} \begin{bmatrix} 1 & 0 \\ 0 & -1 \end{bmatrix} \quad (27)$$

and express the effective Liouvillian in the new basis. The result is:

$$\begin{aligned}L_{\text{eff}} &= L_0 + \mathcal{P}\mathcal{V}\mathcal{Q}\mathcal{G}_0(0)\mathcal{Q}\mathcal{V}\mathcal{P} \\ L_{\text{eff}} - L_0 &= -\frac{i}{\hbar} [H', \cdot] + L^D \\ H' &= \sqrt{2}n\pi V \mu_c \sigma_y\end{aligned}\quad (28)$$

where L_0 is the original Liouvillian in the \mathcal{P} partition, H' is an (Hermitian) addition to the Hamiltonian and L^D is a superoperator in Lindblad form (Eq. (26)). The strictly dissipative part can be completely determined by the coefficients c_{ij} :

$$c_{ij} = \begin{bmatrix} c_3 & ic_3 & c_2 \\ -ic_3 & c_3 & -ic_2 \\ c_2 & ic_2 & c_1 \end{bmatrix} \quad (29)$$

with $c_1 = \Omega^2 + \gamma_{eg}$, $c_2 = \Omega$ and $c_3 = 1 + \Gamma_e$. To check the positivity of the c_{ij} matrix we diagonalize it. The eigenvalues are:

$$\begin{aligned}c_{\pm} = & \frac{1}{2} \left[(\Omega^2 + 2\Gamma_e + \gamma_{eg} + 2) \right. \\ & \left. \pm \sqrt{(\Omega^2 - 2\Gamma_e + \gamma_{eg} - 2)^2 - 8\Omega^2} \right]\end{aligned}\quad (30)$$

Both eigenvalues are positive proving that the matrix is positive definite and that the operator can in fact be written in Lindblad form.

APPENDIX C: ACCOMPANYING SOFTWARE

To make the results of this paper more accessible, we have included all results, equations and plots in an interactive python notebook. The notebook consists of a symbolic part where the expressions that include dissipation from the discrete state and pure decoherence - too

intricate to write in an article - can be obtained. The second part consists of numerical simulations where the plots produced in the paper can be redrawn and where any simulation of the solution to the Fano model can be plotted. The software can be downloaded from fanoqs.wordpress.com.